SOFT-DOCKING SYSTEM FOR CAPTURE OF IRREGULARLY SHAPED, UNCONTROLLED SPACE OBJECTS

F. Branz[1], L. Savioli[1], A. Francesconi [1][2], F. Sansone[1], J. Krahn[3], and C. Menon[3]

[1]*University of Padova, CISAS "G. Colombo", Padova, Italy, Email: francesco.branz@unipd.it, livia.savioli@studenti.unipd.it, alessandro.francesconi@unipd.it, francesco.sansone@studenti.unipd.it*
[2]*University of Padova, Department of Industrial Engineering, Padova, Italy*
[3]*MENRVA Lab, School of Engineering Science, Simon Fraser University, Burnaby, Canada, Email: jkrahn@sfu.ca, cmenon@sfu.ca*

ABSTRACT

Over the last decades, the interest around Active Debris Removal missions grew considerably due to the increasing threat represented by the space debris populating near-Earth orbits. This paper presents the concept of a soft docking system suitable for capture of non-cooperative, large objects regardless of shape, surface features and motion. The innovative concept exploits a compliant electro-dry adhesive surface for mating and a robotic support structure composed by smart-material actuators. The adhesion surface combines electrostatic attraction and van der Waals forces; it is highly flexible and compliant to local irregularities of the target surface. The proposed capture concept increases the operative flexibility, tolerating critical scenario uncertainties (i.e. target shape, motion, mass). The active support structure can be controlled to adapt to the target object external geometry and to damp relative motion between target and chaser. Preliminary analysis was conducted both assessing the expected capture loads and the available adhesion forces.

Key words: space debris capture; electro-adhesion; electro-active polymers.

1. INTRODUCTION

In the last decade, the threat to spaceflight security related to the presence of artificial orbital debris in the near-Earth space environment has arose as one of the most critical issues that governments, space agencies and companies are going to face in the near future. The result of over fifty years of human activities in space is a population of roughly 20000 objects larger than 10 cm, of which about 13500 are tracked. They are composed mainly by fragments due to collisions or third stages separations in LEO and intact but non-operational spacecraft in GEO [23]. However, smaller objects are estimated to be many more, with a less than 1 cm space debris population of the order of hundreds of thousands. The fragments population in LEO increased abruptly a few years ago as a result of two events: the destruction of the Chinese FENG YUN 1C weather satellite in 2007 and the collision between the IRIDIUM and COSMOS spacecraft in 2009. More recently, the Russian satellite Blits was hit by a fragment of FENG YUN 1C and severely damaged, so that its mission is compromised. These events demonstrated what was pointed out by [26]: not only the actual space debris population is a danger for both manned and unmanned missions, but also it could grow so much to prevent any human activities in space in the near future because of a collision cascade (the so called Kessler syndrome). Even in the unrealistic hypothesis of immediate halt of any launch to space, the debris population is not expected to remain stable for more than few decades, and then it will dramatically grow as the breakups due to collisions will exceed the debris loss due to orbital decay. In a more realistic scenario, this phenomenon could occur within a few years. Several mitigation techniques were proposed and are currently adopted with the aim of reducing the debris generation during future space missions; these include, for example, elimination of explosive actuators, venting or depletion of pressurized fluids to prevent accidental over-pressurization and break-up, de-activation of battery charge lines after mission disposal and post-mission orbital decay in less than 25 years. Although strictly necessary, these techniques are perceived as absolutely not sufficient and only Active Debris Removal (ADR) from the most densely populated orbits could effectively prevent their uncontrolled, exponential growth [27]. In particular, large objects which populate low Earth orbits, such as second stages or massive, non-operational spacecraft are seen as the best candidate for active removal missions, since the chance of collision is strictly related to the dimensions of the objects in space and, in the case of a collision they would generate a much larger amount of debris.

A typical ADR mission is composed of four operations: target identification, rendezvous/approach, capture and deorbiting. The most critical technical challenge within such missions is probably represented by the capture subsystem used to connect the target debris with a servicing S/C. An overview of the proposed solutions to capture follows.

1.1. Space capture systems

To date, a variety of grasping concepts for ADR has been studied although none has been flight proven yet. The main concepts proposed in literature are: (1) robotic arms, (2) nets, (3) harpoons, (4) polymeric foams or (5) nozzle probes.

1. Robotic arms have already been employed and validated for several on-orbit operations [6][11] and could represent a suitable option for debris removal. Various solutions for uncontrolled object capture have been proposed: dual-arm systems [29], tentacle based systems [35], capture through standard launcher-payload interfaces [19], fleets of small scale robotic spacecraft [42], robot arms with brush-like end-effectors [30]. DEOS [33] is a German Space Agency mission that aims to capture a client vehicle with a servicing spacecraft by means of a robotic arm that grasps handles on the target object. The main disadvantage of robotic systems is the lack of research on appropriate end-effectors suitable to capture irregular shaped objects without damaging brittle features: robotic capture strategies typically assume that the target object offers structural features of known geometry, capable to withstand the handling loads and compatible with common hand grips.

2. Net based systems offer a large contact surface with the target and a good adaptability to irregular shapes. Nets can be held by some sort of structure (e.g. inflatable [47]) or be thrown towards the target [35][46]. The major drawbacks of this solution come from the extreme flexibility of nets determining a complex deployment-capture dynamics and difficulties in controlling the target after capture.

3. Harpoons [34] can be shot toward the surface of the target, thus being compatible with a variety of objects. This technique is penalized by several operative risks connected mainly with the possible generation of debris at the impact between harpoon and target, with the chance to cause explosions by hitting pressurized vessels or batteries and with the angular momentum transferred to the target at the moment of impact.

4. Polymeric foams as capture/removal system have been proposed according to two different operational concepts. On one hand, such materials can be sprayed towards the debris to achieve chemical bonding regardless of target shape [32]. On the other hand, these foams can also be employed to increase the atmospheric drag of the target object (i.e. ballistic coefficient) by enveloping the debris within a large volume of polymer [1]. The biggest weakness of this approach is connected to the employed material performances in space and its strength when solid.

5. The use of nozzle probes to fit into the target object nozzles have been studied [17][40]. This approach can be applied to a variety of objects and can provide a strong connection with the target. The main disadvantage of this solution is the lack of generality, the need of a non-gimballed target nozzle and the need to identify and align with the nozzle axis in spite of the target tumbling motion.

2. CAPTURE MECHANISM CONCEPT

A new approach is proposed for non-cooperative object capture exploiting adhesive systems. The innovative device proposed is based on two key technologies: electro-dry-adhesion and dielectric Electro-Active Polymers (EAP). The servicing S/C is equipped with a soft-docking mechanism with an innovative surface that establishes electro-dry-adhesion attraction forces with the debris surface. Immediately after contact, the capture forces arise at the interface between the mechanism and the external debris surface and the connection is guaranteed. In order to obtain a good contact with the client object, the adhesive system is designed to be sufficiently flexible and to comply to local irregularities of the target surface. The aim of this research is to realize a device that can be employed in a large variety of ADR missions. For this reason, the capture surface is held by an adaptive robotic structure that is capable of conforming to the target shape, to follow the initial target motion and to damp the relative velocity between target and chaser. The adaptive robotic structure is composed of a number of dielectric EAP actuators. Fig. 1 shows a conceptual sketch of the proposed capture solution.

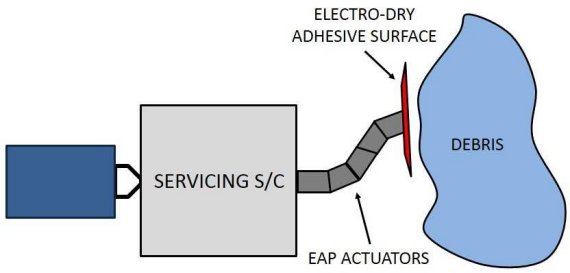

Figure 1. Proposed capture mechanism sketch.

2.1. Electro-dry-adhesive surface

The geckos ability to climb a wide variety of surfaces is thought to be due to van der Waals interactions [3]. The ability of the hierarchical fibres, found on the toe of the gecko, to conform to a surface enables the tips of the fibres to be in the close surface-surface contact necessary for van der Waals interactions to occur. The features which allow geckos to climb on many different structures have inspired the design and fabrication of synthetic dry adhesives for use as attachment systems where strong, fast and reliable adhesion is required [8][15][43]. Inspired by the gecko, many different research groups have pursued various methods of fabricating synthetic dry adhesives including molding or casting of polymers [12][37][38], deep reactive ion etching [13][20][21][22], nano-drawing [14], direct laser writing [36] and E-beam lithography [41]. Using these and other techniques, arrays of uniform nano- or micro-scale fibrillar structures have been fabricated.

In order to achieve optimal adhesion with synthetic dry adhesives, a preloading force is required to force the adhesive into the close surface-surface contact required for van der Waals forces. However, the recent introduction of conductive particles such as Carbon Black (CB) into the polymers which make up the synthetic dry adhesive structures has enabled the use of electrostatic forces to create self-preloading dry adhesives referred to as electro-dry-adhesives [25]. When a high voltage is applied to the electro-dry-adhesives, the op-

positely charged electrodes induce an opposing charge on the substrate they are attaching to. The generated electrostatic charge acts on the electro-dry-adhesives with a preloading force and ensures good adhesive contact.

Electro-dry-adhesives synergistically combine the use of synthetic gecko-like dry adhesives with the ability to self-preload using self-generated electrostatic forces. The generated electrostatic force, F, is described by [18]:

$$F = \frac{A\epsilon_0 V^2}{2\left(l + \frac{2d}{\epsilon_r}\right)^2} \quad (1)$$

where A is the area in contact, V is the applied voltage, l is the separation between electrodes, d is the thickness of the dielectric layer ϵ_r is the relative permittivity and ϵ_0 is the dielectric permittivity of vacuum. As can be seen in Eq. 1, increasing the applied voltage results in a voltage squared increase in the generated electrostatic force. The proposed attachment system for the cleaning up of space debris would be composed of multiple electro-dry-adhesive contact areas with opposing charges as shown in Fig. 2. When a voltage is applied to the electro-dry-adhesives, they are electrostatically attracted to the attachment substrate (space debris). The electro-dry-adhesives would then form a passive van der Waals adhesive bond with the space debris and the voltage could be removed to conserve power while remaining attached.

Figure 2. Proposed electro-dry-adhesive attachment mechanism for space junk removal.

2.2. Electro-active polymer actuator

A large number of interesting EAPs have been studied and partially characterized so far [4]. Among them it is possible to identify two main categories: ionic EAPs, such as polymer gels, conjugated polymers, carbon nanotubes polymers, and electronic EAPs, such as piezoelectric polymers, electrostrictive polymers, dielectric elastomers. The latter show the best performances and appear to be suitable for the development of actuators. As a matter of fact, a number of actuators based on dielectric elastomers is described in literature with various shapes and geometries [5][16][24][31], some of them conceived for space use [2]. The working principle of dielectric elastomers is very simple. They are usually manufactured as thin membranes on whose surfaces flexible electrodes are applied. This assembly acts as a compliant capacitor where the elastomer membrane acts as dielectric material. The application of a voltage between the two polymer faces determines the charging of the device; consequently, due to the Maxwell forces that arise inside the capacitor, the membrane thickness reduces while its planar dimensions increase. It has been demonstrated that the application of a certain amount of pre-stretch to the elastomer increases considerably its deformation capability. The deformation capability can be exploited to manufacture different actuators with various geometries and, consequently, degrees of freedom. The major drawback of the use of such materials is the need of high voltage values (4 - 7 kV) for actuation.

The proposed robotic structure is composed by a number of 2-DoF actuators connected in series obtaining a redundant robotic arm with distributed actuation. The single actuator represents the elementary unit of the robotic system and this work focuses on its preliminary analysis and defining the requirements. The proposed device is based on dielectric polymer elements and is designed to be lightweight, low power consumption and to have no mobile mechanical coupling (e.g. ball bearings). In each actuator, a rigid rod is moved from its nominal position by the deformation of the polymeric film elements. Other rigid components connect the rod to the deformable elements and the actuator body to ground. The dielectric polymer action is exploited to obtain two rotational degrees of freedom about the two axes perpendicular to the actuator rod. Since the device motion is generated by deformable elements, the angular deflection of the actuator is intrinsically limited. A maximum total deflection value of 90 deg is considered and the actual value for each single device depends on the number of actuators composing the robotic system. Three concurrent geometries are considered at this point for the generation of the desired motion (see Fig.3, active elements in green, rigid components in dark grey):

1. cylindrical configuration: the polymer film is wrapped in two cylinders which are axially pre-stretched
2. planar configuration: a circular film element is radially pre-stretched
3. double-cone configuration: two polymer film discs are deformed by pulling in the middle and, consequently, shaped as cones

In all three cases axial-symmetric, pre-stretched, polymeric elements are employed. A compliant conductive material (e.g. carbon grease) is deposited on the polymer surface forming different electrodes. The characteristic symmetric distribution of electrodes on the polymer allows the activation of only some portions of the material. With this approach it is possible to obtain the differential deflection of the rod about the two axes and generate the desired actuation. Applying high voltage to the electrodes produces a reduction of the polymer thickness and an in-plane elongation of the film mainly due to the stresses determined by the initially imposed pre-stretch condition. In the first configuration the applied voltage locally increases the cylinder height; in the planar configuration the polymer film is radially deformed by the actuation; in the double-cone the actuation forces locally extend the cone side. Multi-layer configuration will be considered to increase the actuation forces.

Since the device has to be controllable within a feedback loop, an angular position determination system will be developed and embedded in the device. This sensor will determine the electrodes capacitance variation across the polymer film as a measure of the membrane thickness reduction and is useful for the reconstruction of the element deformed shape.

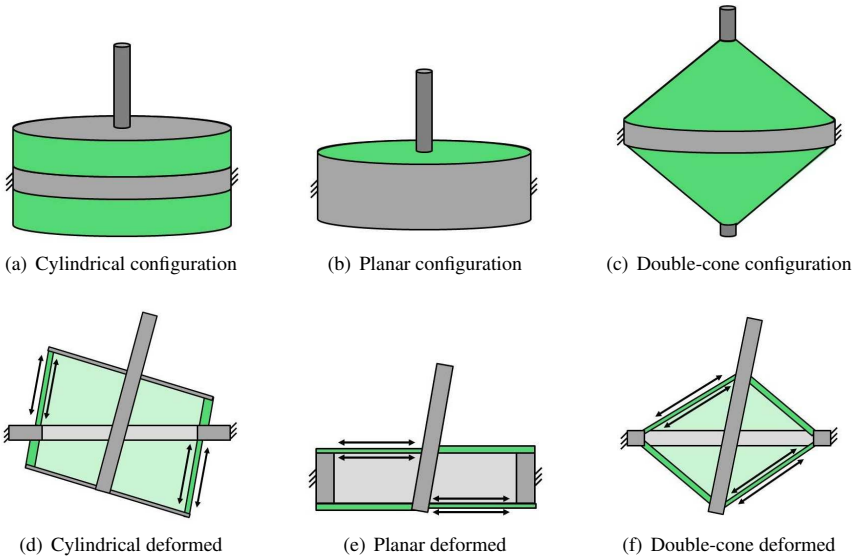

(a) Cylindrical configuration (b) Planar configuration (c) Double-cone configuration

(d) Cylindrical deformed (e) Planar deformed (f) Double-cone deformed

Figure 3. Concurrent actuator geometries considered for future development (a, b, c). Section views of deformed geometries (d, e, f).

2.3. Capture strategy

The general idea behind the ADR mission conceived to employ the proposed capture system is that a small (< 200 kg) servicing spacecraft performs rendezvous to a relevant debris object, approaches and captures it; finally, once the whole system attitude is stabilized, de-orbiting is performed by means of an electric propulsion system carried on board the chaser spacecraft. The adhesive system most critical aspect are the low available capture forces, thus determining the necessity to limit the peak forces occurring during the docking sequence. Two different capture strategies have been identified in order to assess the capture forces reductions, referring to the pre- and post-capture desired motion of the whole system.

The first strategy focuses on the pre-capture sequence: if the supporting robotic arm is capable of following the desired capture point on the target surface during approach, the impulsive forces at the moment of contact are considerably reduced. This type of manoeuvre requires the chaser vehicle having the capability to determine the motion of the target and guide the adhesive surface towards the designated connection point, thus minimizing the relative velocity between the two interface surfaces. Lower loads are applied to the contact interface at the cost of more resources required to the chaser platform.

The second considered strategy refers to the post-capture control strategy. The aim to damp or store the residual angular momentum carried by the debris can be achieved with two opposite approaches:

1. the servicing S/C can be kept fixed at nominal attitude by means of its Attitude Control System (ACS) and the angular momentum can be properly distributed to the different ACS actuators (e.g. reaction wheels) of the satellite
2. the servicing S/C can be completely uncontrolled and allowed to follow the motion of the debris; the capture system dampens the relative motion between the S/C and the debris until the system rotates rigidly

Since the mass of the servicing S/C is considerably lower compared to that of the debris, the second approach determines lower capture forces, as will be clear from the results. Therefore, the second approach requires both less adhesion strength and more relaxed control performances to the chaser ACS.

2.4. Advantages of the proposed solution

The described device avoids the limits of other solutions currently evaluated in literature for non-cooperative space objects capture. In particular, the proposed concept offers a large operative flexibility which is a key feature in the debris capture problem, given the strong uncertainties derived from the mission scenario (e.g. target inertia, geometry and motion). The combination of the adhesive technology and the robotic controllable support structure allows it to mate with virtually any type of surface, to tolerate relative motion between the capture mechanism and the target at the moment of capture and to control the entire system dynamics and attitude. The adhesive capture does not require any particular feature on the target body to be performed, thus being generally applicable to dock with any object. A considerable amount of contact surface is available and, consequently, lower local loads are transmitted to the target debris reducing the risk of ruptures and further debris generation. A high controllability and manipulability of the debris after capture is possible thanks to the robotic arm and the use of deformable polymeric elements which also provide the capability to passively damp a portion of the system kinetic energy.

3. EXAMPLE MISSION SCENARIO

In order to perform a preliminary analysis simulation campaign, an example mission scenario is selected. The capture strategy is described in Sec. 2.3, while here the debris selection and the servicing S/C sizing are presented.

3.1. Target selection, features and motion

With broad consensus among the international space community [27][28], the most interesting targets for active debris removal are identified as large, intact objects located in highly populated regions of space, since they are a potential source of numerous debris. In particular, rocket launcher upper stages appear to be good candidates for ADR missions for several reasons [9]. First, these objects are characterized by large mass and, if destroyed by an impact, would generate countless dangerous fragments. Second, they usually have a regular shape and, consequently, capture is easier. Third, they do not present any fragile appendage or structure protruding from the main body; such features could collide with the servicing S/C during approach/capture or they could detach from the main body and become a new piece of debris. Fourth, they are numerous and similar to each other allowing to employ the same capture system over a number of different missions with no or only minor modifications. Fifth, some particular objects in this class (e.g. COSMOS-3M second stages) are fairly uniformly distributed on a large variety of orbital bands, making it possible to perform a distributed removal action with few mission scenario differences.

For the example mission scenario proposed in this work, the mentioned COSMOS-3M rocket second stage is selected as possible target. The object mass ($\sim$1400 kg) is representative of a large variety of objects of the same class (i.e. Vostok, Ariane 1 & 4). The object shape is roughly cylindrical (diameter 2.4 m, length 6.5 m) and the external surface is pretty regular and solid, thus being suitable for adhesive capture.

A critical aspect of debris capture is the determination and management of the object attitude motion. The capture system requirements are strongly dependent on the object angular rate at the moment of connection, both in terms of impulsive capture forces as well as angular momentum management. In general, the objects spin rate is unknown and, although studies exist aiming to determine it in order to ease the ADR procedures [7], different values of possible residual angular velocities have to be considered during simulation in order to determine the capture system requirements. To identify a realistic range of possible angular rates, different scenarios are considered. The COSMOS-3M second stage is nominally not spinned, but on some missions a small solid rocket motor placed toward aft fires within seconds after payload separation and gives the spent stage a rotational motion that increases the distance from the released payload. A rough estimate of the residual angular rate in this case is $< 10^{-2} \frac{\text{rad}}{\text{s}}$ assuming 1 s of burning time, 20 N of thrust and 2 m of moment arm. In the case that no rocket is fired to ease payload separation, a possible motion condition for the object is the oscillation around the gravity gradient equilibrium position; a simple long term simulation has been performed to determine the maximum angular velocity under gravity gradient torques for a COSMOS second stage on a 80 deg inclined, 700 km LEO orbit. The resulting maximum angular velocity is $< 10^{-4} \frac{\text{rad}}{\text{s}}$.

3.2. Servicing S/C preliminary sizing

The general idea is to keep the ADR mission as simple and low-cost as possible, in order to increase the effectiveness and sustainability of the debris remediation technique. For this reason, in the hypothetical mission scenario simulated here, a S/C in the micro/small satellite range is selected. A preliminary sizing of the servicing vehicle was conducted in order to determine its geometric and inertial properties. The de-orbiting system adopted is based on electric propulsion and was sized as suggested by [39]. Historical data and preliminary design relations [44] were employed for the spacecraft bus sizing that included the following main subsystems: structure, power, ACS and communication. The breakdown of masses of the satellite bus, the re-entry system and the capture system is presented in Tab. 1. The overall vehicle mass is 107 kg including a 20% margin, resulting in a cubic shaped S/C body with a side length of approximately 0.7 m.

Table 1. Servicing S/C masses

System	Mass [kg]
Spacecraft bus	50
Re-entry system	51
Capture system	6

4. PRELIMINARY ANALYSIS

The main system components (adhesive surface and EAP actuator) performances are assessed at the basic level to determine the operation requirements in terms of loads (i.e. torques and forces).

4.1. Numerical dynamics simulations of capture

The simulations performed assess the dynamics of the combined debris-chaser system starting from the moment of capture. The system is modelled as a combination of a variable number of bodies (i.e. debris, S/C, actuators) connected to each other by means of two-axis rotational joints that represent the actuators degrees of freedom. A control torque is applied to each actuator.

In order to determine the actuator required torque, a control law has to be selected. For simplicity a PD control is implemented in this preliminary phase. The proportional and derivative gains are sized by imposing an appropriate rising time to the system step response in order to avoid an arm deflection greater than 90 deg (see Sec. 2.2). Also, to ensure that the controlled system is stable, a minimum 45 deg phase margin is imposed. With this approach the control law gains

are dependent on the initial value of angular momentum carried by the debris.

Referencing Section 2.3, different simulation approaches are adopted to account for the different capture strategies conceived. To simulate the first strategy where the satellite is nominally fixed, the S/C body is constrained to having no motion allowed. The second strategy is simulated assuming that the debris motion is not modified by the connection with the servicing spacecraft. These two simulation approaches introduce a simplification to the system and, therefore, accuracy is somewhat affected. Nevertheless, the simulations are for extreme situations which represent the worst load case scenarios. In addition, all simulations are performed twice, assuming that initially the robotic arm is both able and unable to follow the motion of the debris during the approach.

A number of simulations are performed with variable values for the initial debris angular momentum. From the estimations presented in Sec. 3.1, the variability range of the angular velocity, ω_{db}, is selected between 10^{-4} and 10^{-1} $\frac{\text{rad}}{\text{s}}$ (including confidence margin).

4.2. Simulation results: requirements on the actuators and adhesives

The simulations provided interesting and useful results for the requirements of the capture system, particularly focusing on the maximum loads applied to the adhesive and robotic system during the capture sequence. The torque, T_{max}, required by the single robotic actuator in order to brake the debris rotation and the shear load, S_{max}, on the adhesive interface are strongly dependent on the initial angular momentum of the debris, $H = \omega_{\text{db}} I_{\text{db}}$. The first approximation on the relations between H and T_{max} or S_{max} is shown in Eq. 2

$$\begin{aligned} T_{\text{max}} &= a_2 H^2 \\ S_{\text{max}} &= b_2 H^2 \end{aligned} \tag{2}$$

where a_2 and b_2 are proper coefficients that depend on the type of simulation executed (i.e. capture strategy, number of robotic actuators and robotic arm approach control). Table 2 shows the simulation results including the normal force load on the adhesive surface. Columns 1 to 3 give information on the type of simulation executed. The first column indicates the capture strategy adopted: if the servicing vehicle is kept fixed or if it is free to move together with the debris. The second column reports the number of actuators in the robotic arm. The third column indicates if the arm is initially still or following the debris rotation. The last three columns give the actual results T_{max}, S_{max} and N_{max} which is the adhesive force required in the direction normal to the adhesive interface. The values in the table are computed with an initial debris angular velocity ω_{db} of 0.1 $\frac{\text{rad}}{\text{s}}$ resulting in an initial debris angular momentum equal to $H_{\text{db}} = 1567$ Nms.

4.3. Expected adhesive shear and normal forces

The shear adhesive strength of the electro-dry-adhesives was measured using a spring scale as shown in Fig. 4. A DC power supply was attached to a DC-DC voltage converter (EMCO, E101CT) to produce the high voltages used during testing. The electro-dry-adhesive sheets were placed gently on a thin ($\sim$110 μm thick) polypropylene sheet securely attached to a steel backing layer. The lateral separation distance between the positive and negatively charged electro-dry-adhesives was 1 cm for all tests. The electro-dry-adhesives surface area was 2.07×10^{-3} m^2. After placing the electro-dry-adhesive sample on the polypropylene sheet, a high voltage was applied while the spring scale was used to measure the shear adhesion force. To measure the normal adhesion pressure, a similar test setup was used except the adhesion pressure was measured normal to the top surface of the electro-dry-adhesive. The measured shear and normal adhesion strengths for 0, 2, 4 and 6 kV are shown in Fig. 5. The error bars indicate the error in measurement. These results

Table 2. Maximum actuation on the robotic arm (T_{max}) and loads on the adhesive (S_{max}, N_{max})

S/C attitude	Act. number	Arm motion	T_{max} [Nm]	S_{max} [N]	N_{max} [N]
fixed	1	still	492	129	224
fixed	2	still	984	4197	208
fixed	3	still	1476	6534	201
fixed	1	follow	492	129	224
fixed	2	follow	492	128	216
fixed	3	follow	492	127	213
free	1	still	4.1	5.4	7.5
free	2	still	8.1	34.6	8.8
free	3	still	12.2	53.9	9.5
free	1	follow	4.1	5.4	7.5
free	2	follow	4.5	5.2	6.9
free	3	follow	4.7	5.1	6.7

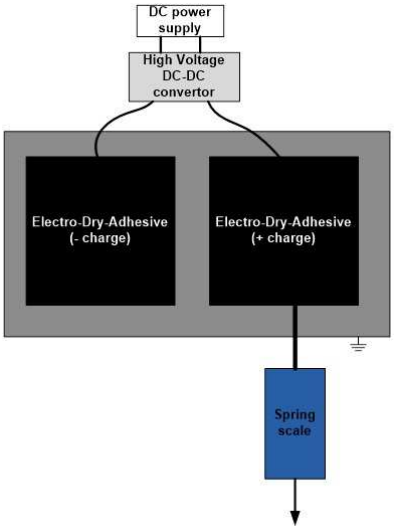

Figure 4. Test setup used to determine the shear adhesion force of the electro-dry-adhesives.

are compatible with the desired adhesion forces presented in Sec. 4.2 which can be achieved with a small adhesive area ($\ll 1$ m^2).

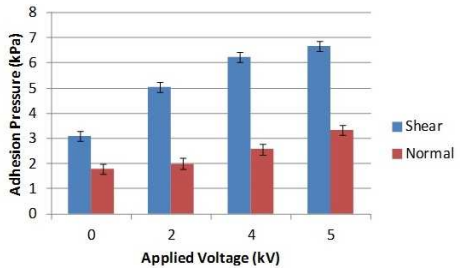

Figure 5. The shear and normal adhesion pressure with estimated error measured for the electro-dry-adhesives placed on a polypropylene sheet with a steel backing layer.

5. CONCLUSION

The present paper described an innovative concept for a capture mechanism suitable for application to ADR space missions. The system exploits electro-dry-adhesive technology to establish the contact with the target debris and features a robotic arm based on EAP actuators for adhesive surface positioning, relative motion control and debris manipulation. Such a capture device increases considerably the operative flexibility of ADR missions by enabling the capture of a wide range of objects with various shape, material, mass and motion characteristics. The concept design of the two core system components (i.e. adhesive surface and EAP actuator) is described and the preliminary analysis results on required torques to the actuators and expected adhesion forces are presented. Dynamical simulations showed a strong dependency of torques and forces from the capture scenario and strategy adopted: in particular, the loads on the system are larger if the debris angular momentum is larger, if the chaser S/C attitude is kept stable and if the robotic arm does not follow the debris motion at the moment of capture.

The first result that can be inferred form the data collected in Tab. 2 is that a free attitude strategy for the chaser S/C is clearly preferable, meaning that the S/C attitude is not controlled during capture and the vehicle is free to move with the target. With this assumption it appears possible to capture an object of the selected class with an adhesive surface area of maximum 10^{-2} m^2 (assuming 2 kV of applied voltage). The arm capability to follow the debris motion helps reducing the loads, particularly in the case of multiple robotic actuators. As a matter of fact, more actuators provide a better mobility to the robotic arm although the required control torque may increase. In general, the actuators are required to provide $5 \div 15$ Nm of torque. A suitable case for the definition of system requisites is the capture of a 1400 kg cylindrical shaped piece of debris rotating at 10^{-1} $\frac{\text{rad}}{\text{s}}$ by means of a chaser S/C with free attitude and equipped with a robotic arm that is capable to follow the debris motion. This type of object is representative of a large number of suitable ADR candidates such as the COSMOS-3M second stages. In this scenario, regardless of the number of robot joints, the required adhesive surface area is $< 5 \times 10^{-3}$ m^2 (2 kV) and the EAP actuators are required to provide < 5 Nm of control torque.

REFERENCES

1. Andrenucci M., Pergola P., Ruggiero A. (2011). Active Removal of Space Debris - Expanding foam application for active debris removal - Final Report
2. Artusi M., Potz M., Aristizabal J. *et al.* (2011). Electroactive Elaastomeric Actuators for the Implementation of a Deformable Spherical Rover. *IEEE/ASME Transactions on Mechatronics*, **16**, 50–57
3. Autumn K., Sitti M., Liang Y. A. *et al.* (2002). Evidence for van der Waals adhesion in gecko setae. *Proceedings of the National Academy of Sciences of the United States of America*, **99**, 12252–6
4. Bar-Cohen Y. (2004). Artificial Muscles using Electroactive Polymers (EAP): Capabilities, Challenges and Potential.
5. Brochu P., Pei Q. (2010). Advances in Dielectric Elastomers for Actuators and Artificial Muscles. *macromolecular Rapid Communications*, **31**, 10–36
6. Caron M., Mills I. (2012). Planning and Execution of Tele-Robotic Maintenance Operations on the ISS. *Proceedings of SpaceOps 2012, Stockholm, Sweden*
7. Cowardin H., Ojakangas G., Mulrooney M. *et al.* (2012). Optical signature analysis of tumbling rocket bodies via laboratory measurements. *Proceedings of the Advanced Maui Optical and Space Surveillance Technologies (AMOS) Conference*
8. Del Campo A., Greiner C., Arzt E. (2007). Contact shape controls adhesion of bioinspired fibrillar surfaces. *Langmuir: the ACS journal of surfaces and colloids*, **23**, 10235–43
9. De Luca L. T., Bernelli F., Maggi F. (2012). Active space debris removal by hybrid engine module. *Proceedings of the 63rd International Astronautical Congress*, Naples, Italy
10. Dimitrov D.N., Yoshida K. (2004). Momentum Distribution in a Space Manipulator for Facilitating the Post-Impact Control. *Proceedings of 2004 IEEE/RSJ International Conference on Intelligent Robots and Systems*, Sendai, Japan
11. Dupuis E., Martin E. (2012). An Overview of the Recent Canadian Space Agency Ativities in Space Robotics. *International Symposium on Artificial Intelligence, Robotics and Automation in Space*, Turin, Italy
12. Glassmaker N. J., Himeno T., Hui C.-Y. *et al.* (2004). Design of biomimetic fibrillar interfaces: 1. Making contact. *Journal of the Royal Society, Interface / the Royal Society*, **1**, 23–33
13. Hui C.-Y., Glassmaker N. J., Tang T. *et al.* (2004). Design of biomimetic fibrillar interfaces: 2. Mechanics of enhanced adhesion. *Journal of The Royal Society Interface*, **1**, 35–48
14. Jeong H. E., Lee S. H., Kim P. *et al.* (2006). Stretched polymer nanohairs by nanodrawing. *Nano letters*, **6**, 1508–13

15. Jeong H. E., Suh K. Y. (2009). Nanohairs and nanotubes: Efficient structural elements for gecko-inspired artificial dry adhesives. *Nano Today*,**4**, 335–46

16. Jung K., Kim K. J., Choi H. R. (2007). A self-sensing dielectric elastomer actuator. *Sencors and Actuators A*, **143**, 343–351

17. Kaiser C., *et al.* (2008). SMART-OLEV An orbital life extension vehicle for servicing commercial spacecrafts in GEO. *Acta Astronautica*, **63** 400–410

18. Karagozler M. E., Campbell J. D., Fedder G. K., *et al.* (2007). Electrostatic latching for inter-module adhesion, power transfer, and communication in modular robots. *2007 IEEE/RSJ International Conference on Intelligent Robots and Systems*, 2779–86

19. Kelm B. E., Angielski J. A., Butcher S. T. *et al.* (2008). FREND: Pushing the Envelope of Space Robotics. *Space Research and Satellite Technology*, 239–241

20. Kim S., Sitti M. (2006). Biologically inspired polymer microfibers with spatulate tips as repeatable fibrillar adhesives. *Applied Physics Letters*, **89**, 261911

21. Kim S., Sitti M., Hui C.-Y. *et al.* (2007). Effect of backing layer thickness on adhesion of single-level elastomer fiber arrays. *Applied Physics Letters*, **91**, 161905

22. Kim S., Sitti M., Xie T. *et al.* (2009). Reversible dry micro-fibrillar adhesives with thermally controllable adhesion. *Soft Matter*, **5**, 3689

23. Klinkrad H., Johnson N. L. (2009). Space Debris Environment Remediation Concepts. *Proceedings of the 5th European Conference on Space Debris*, Darmstadt, Germany

24. Kovacs G., Ha S. M., Michel S. *et al.* (2008). Study on core free rolled actuator based on soft dielectric EAP. *Proceedings of SPIE*, **6927**, Smart Structures and Materials: Electroactive Polymer Actuators and Devices (EAPAD)

25. Krahn J., Menon C. (2012). Electro-Dry-Adhesion. *Langmuir*, **28**, 5438–43

26. Liou J.-C., Johnson N. L. (2008). Instability of the present LEO satellite populations. *Advances in Space Research*, **41**, 1046–1053

27. Liou J.-C., Johnson N. L. (2009). A sensitivity study of the effectiveness of active debris removal in LEO. *Acta Astronautica*, **64**, 236–243

28. Liou J.-C., Johnson N. L., Hill N. M. (2010). Controlling the growth of future LEO debris populations with active debris removal. *Acta Astronautica*, **66**, 648–653

29. Miyabe T., Konno A., Uchiyama M. (2003). Automated Object Capturing with a Two-Arm Flexible Manipulator. *Proceedings of the IEEE International Conference on Robotics and Automation*, 2529-2534, Taipei, Taiwan

30. Nishida S., Kawamoto S. (2011). Strategy for Capturing of a Tumbling Space Debris. *Acta Astronautica*, **68**, 113-120

31. Pei Q., Rosenthal M. A., Pelrine R. *et al.* (2003). Multifunctional electroelastomer roll actuators and their application for biomimetic walking robots. *Proceedings of SPIE*, **5051**, Smart Structures and Materials: Electroactive Polymer Actuators and Devices (EAPAD)

32. Piergentili F., Candini G. P., Piattoni J. *et al.* (2011). Redemption: a Microgravity Experiment to Test Foam for Space Debris Removal. *Proceedings of the 62nd International Astronautical Congress*, Cape Town, South Africa

33. Rank P., Mühlbauer Q., Naumann W. *et al.* (2011). DEOS Automation and Robotics Payload. *Proceedings of the 11th Symposium on Advanced Space Technologies in Robotics and Automation* ESA/ESTEC, Noordwijk

34. Reed J., Busquets J. White C. (2012). Grappling System for Capturing Heavy Space Debris. *2nd European Workshop on Active Debris Removal* Paris, France

35. Robotic Geostationary orbit Restorer (ROGER): `http://www.esa.int/TEC/Robotics/SEMTWLKKKSE_0.html`

36. Rhrig M., Thiel M., Worgull M. *et al.* (2012). 3D direct laser writing of nano- and microstructured hierarchical gecko-mimicking surfaces. *Small (Weinheim an der Bergstrasse, Germany)*, **8**, 3009–15

37. Sameoto D., Menon C. (2009). A low-cost, high-yield fabrication method for producing optimized biomimetic dry adhesives. *Journal of Micromechanics and Microengineering*, **19**

38. Sameoto D., Menon C. (2009). Direct molding of dry adhesives with anisotropic peel strength using an offset lift-off photoresist mold. *Journal of Micromechanics and Microengineering*, **19**, 115026

39. Savioli L., Francesconi A., Maggi F. *et al.* (2013). Space debris removal using multi-mission modular spacecraft. *Proceedings of the 6th European Conference on Space Debris*, Darmstadt, Germany

40. Trushlyakov V., Shalay V., Shatrov J. *et al.* (2009). ctive De-orbiting Onboard System from LEO of Upper Stages of Launchers. *Proceedings of the 5th European Conference on Space Debris*, Darmstadt, Germany

41. Tsai Y.-C., Shih W.-P., Wang Y.-M. *et al.* (2006). E-Beam Photoresist and Carbon Nanotubes as Biomimetic Dry Adhesives. *Proceedings of the 19th IEEE International Conference on Micro Electro Mechanical Systems*, 926–9

42. Ueno H., Dubowsky S., Lee C. *et al.* (2002). Space Robotic Mission Concepts for Capturing Stray Objects. *Proceedings 23rd Space Symposium on Space Technology and Science*, Matsue, Japan

43. Varenberg M., Gorb S. (2008). Close-up of mushroom-shaped fibrillar adhesive microstructure: contact element behaviour. *Journal of the Royal Society, Interface / the Royal Society*, **5**, 785–9

44. Wertz J. R., Larson W. J. (editors)(1999). *Space Mission Analysis and Design*. Microcosm Press and Kulver Academic Publishers, ed. 3

45. Wissler M., Mazza E. (2006). Mechanical behavior of an acrylic elastomer used in dielectric elastomer actuators. *Sensors and Actuators A*, **134**, 494–504

46. Zhai G., Zhang J. (2012). Space Tether Net System for Debris Capture and Removal. *4th International Conference on Intelligent Human-Machine Systems and Cybernetics* Nanchang, China

47. Zinner N., Williamson A., Brenner K. *et al.* (2011). Junk Hunter: Autonomous Rendezvous, Capture, and Deorbit of Orbital Debris. *Revolutionary Aerospace Systems Concepts Academic Linkage (RASC-AL) Conference*